



Cite this: *Chem. Commun.*, 2024, 60, 2228

Received 25th December 2023,
Accepted 26th January 2024

DOI: 10.1039/d3cc06264c

rsc.li/chemcomm

Insights into non-covalent interactions in dicopper(II,II) complexes bearing a naphthyridine scaffold: anion-dictated electrochemistry†

Jonathan De Tovar, * Christian Philouze, Aurore Thibon-Pourret and Catherine Belle

A family of bis(μ -hydroxido)dicopper(II,II) complexes bearing a naphthyridine-based scaffold has been synthesized and characterized. Cyclic voltammetry reveals that the nature of the anions present in the complexes plays a pivotal role in their electrochemical properties. X-ray diffraction, spectroscopic and electrochemical analysis data support the formation of intimate ion pairs by non-covalent interactions driving to a ca. 270 mV difference for the potential required to mono-oxidize the Cu^{II}Cu^{II} species.

Non-covalent interactions^{1,2} have been shown to play a pivotal role in the science of intermolecular relationships in chemistry³ and biology,⁴ such as protein folding^{2,5} and chiral recognition.⁶ Beyond classic hydrogen bond and van der Waals forces, non-covalent π interactions and C–F \cdots H–C interactions^{7,8} have attracted the attention of the research community, since these forces are key control parameters involved in a variety of chemical transformations such as asymmetric transfer hydrogenations.⁶ Additionally, many of these chemical transformations are not only assisted by intra-molecular non-covalent interactions but also inter-molecular, which promotes the formation of ion pairs with interesting properties. Recently, it has been evidenced that the redox process associated with the ferrocenium/ferrocene couple ($\text{Fc}^{+/\circ}$) is dependent on the nature of the anion present in the electrolyte due to the Fc^+ –anion ion pair interaction and steric constraints, which modulate the interfacial properties.⁹ Within this context, Kim and Yokota and co-workers observed that the potential associated for such a redox event can vary between 30 and up to 170 mV depending on the nature of the anion present in the medium. However, although these interactions offer a tuning possibility for building structure–activity relationships in catalysts, direct incorporation of specific π interactions into the design of molecular

systems with precise control and reactivity remains a pivotal challenge.

We have initiated studies aimed at building and identifying catalytic systems in which these weak, yet important non-covalent interactions, could open new routes to enable challenging chemical transformations like selective C–H bond activation. Within this context and inspired by nature, Belle *et al.* found that dicopper(II,II) complexes containing a dipyridylethane naphthyridine hexadentate ligand not only act as a good compartmental ligand while allowing the isolation of dinuclear copper(II,II) complexes keeping the metallic centers in close proximity,¹⁰ but also have been demonstrated to activate toluene under electrochemically and environmentally friendly conditions.¹¹

We envisioned, thus, that non-covalent interactions could purposefully be used as dicopper(II,II) design tools for tuning both their oxidation potential and 2nd sphere effects, particularly when using tighter cages than the dipyridylethane naphthyridine ligand. For this purpose, a di((3,5-dimethyl)pyrazolyl)methane naphthyridine ligand (**L**) has been synthesized based on the Skraup–Doebner–von Miller quinoline synthesis¹² starting with **1** and crotonaldehyde (**2**) yielding **3** followed by a subsequent oxidation of the methyl moieties into carboxaldehyde groups (compound **4**) mediated by SeO_2 (Scheme S1, ESI†).¹² After synthesizing the dicarboxaldehyde–naphthyridine scaffold, bis(3,5-dimethylpyrazol-1-yl)methanone (**5**)¹³ was condensed with the former yielding ligand **L** (Scheme S1, ESI†). Then, three dicopper(II,II) molecular complexes named **C1**·(ClO_4)₂, **C1**·(BF_4)₂ and **C1**·(OTf)₂ (where $\text{OTf}^- = \text{CF}_3\text{SO}_3^-$) have been synthesized (Scheme 1) allowing the evaluation of (i) the coordination properties of this ligand, (ii) the oxidative potential of the as-synthesized complexes for the couple $E^{1/2}(\text{Cu}^{\text{III}}\text{Cu}^{\text{II}}/\text{Cu}^{\text{II}}\text{Cu}^{\text{II}})$ and (iii) their stabilities under ambient conditions.

Suitable crystals for **C1**·(ClO_4)₂, **C1**·(BF_4)₂ and **C1**·(OTf)₂ were obtained, crystallizing in the triclinic and orthorhombic space groups for the first two and the latter, respectively (see Table S1, ESI†). On the one hand, the molecular plots obtained (Fig. 1) evidence that the anions stay in the 2nd coordination sphere

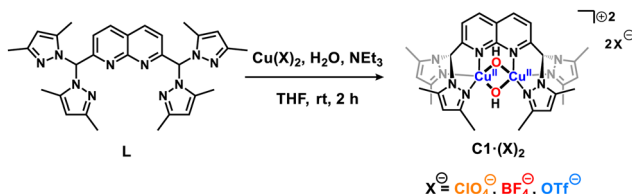
Université Grenoble Alpes, CNRS, DCM, UMR 5250, 38000 Grenoble, France.

E-mail: Jonathan.De-Tovar@univ-grenoble-alpes.fr

† Electronic supplementary information (ESI) available. CCDC 2312255–2312259.

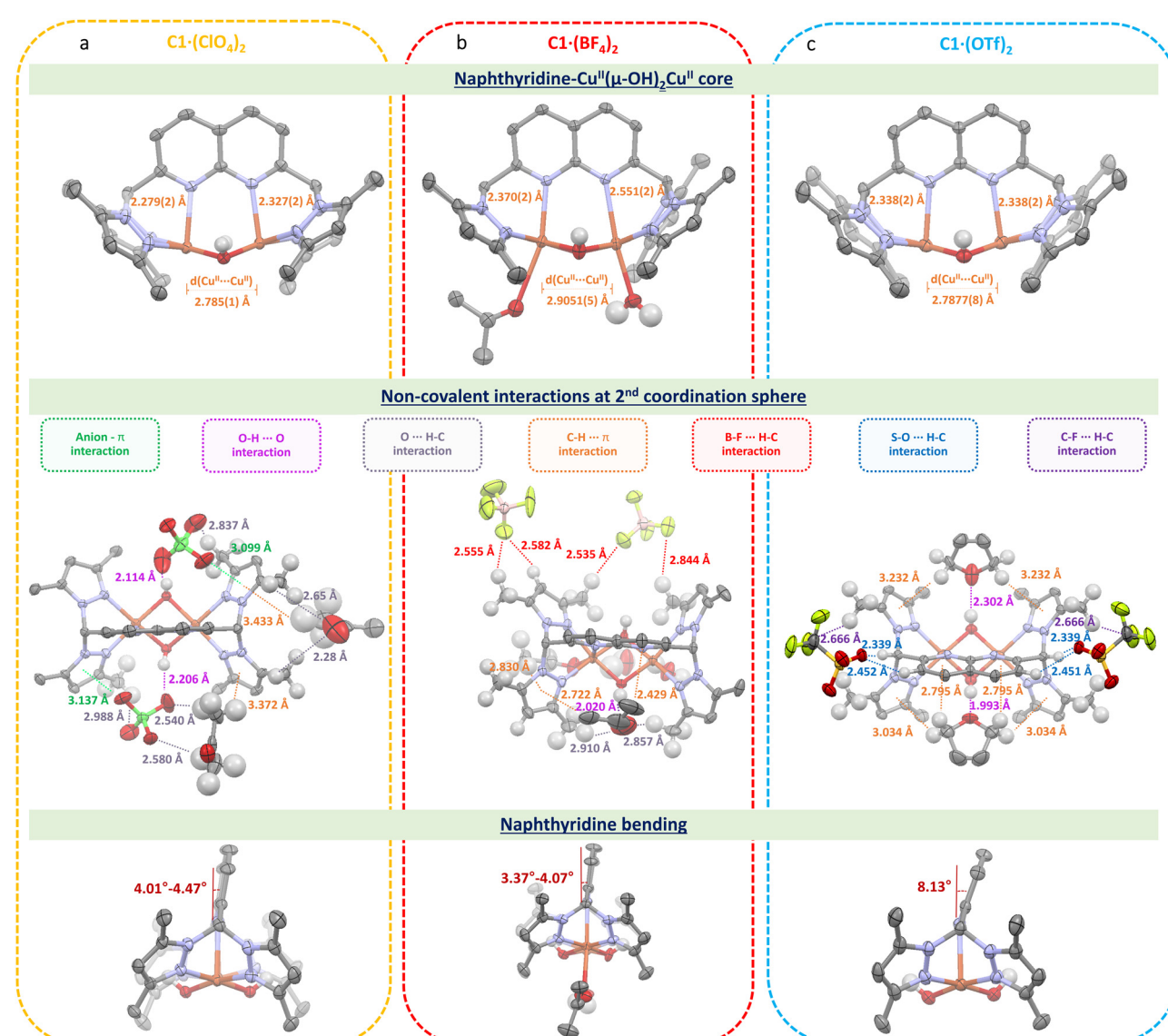
For ESI and crystallographic data in CIF or other electronic format see DOI: <https://doi.org/10.1039/d3cc06264c>



Scheme 1 Synthesis of $\mathbf{C1}\cdot(\mathbf{X})_2$ complexes prepared in this work.

contrary to the previously reported dipyridylethane naphthyridine-based dicopper(II,II) complex, in which one triflate is coordinated to one copper(II) center in the solid-state.¹⁰ Instead, the ClO_4^- , BF_4^- and OTf^- anions establish non-covalent interactions (hydrogen bonding, anion- π , C-H \cdots π , B-F \cdots H-C and C-F \cdots H-C) with the $\mathbf{C1}^{2+}$ scaffold, where the

position of the anions nearby $\mathbf{C1}^{2+}$ is governed by the nature of the former and the structure of the latter. Additionally, ligand **L** bears methyl-enriched pyrazole moieties, which lead to a dissimilar 2nd coordination sphere shell compared to the previously reported complex,¹¹ making the presence of non-covalent interactions a pivotal factor to stabilize such complexes. On the other hand, although all complexes exhibit a dicopper bis(μ -hydroxido) core, the $\text{Cu}\cdots\text{Cu}$ and $\text{Cu}\cdots\text{N}_{\text{naph}}$ (where naph = naphthyridine) bond lengths are rather similar for $\mathbf{C1}\cdot(\text{ClO}_4)_2$ and $\mathbf{C1}\cdot(\text{OTf})_2$ but longer for $\mathbf{C1}\cdot(\text{BF}_4)_2$. These variations can be attributed to the distinct hydrophobic and interactive nature of the anions. While ClO_4^- establishes not only anion- π interactions but also hydrogen bonds, as observed for OTf^- , the latter, due to its perfluorinated methyl chain, locates itself in the less polar region of the $\mathbf{C1}^{2+}$ scaffold. In

Fig. 1 Displacement ellipsoid plots of (a) $\mathbf{C1}\cdot(\text{ClO}_4)_2$, (b) $\mathbf{C1}\cdot(\text{BF}_4)_2$ and (c) $\mathbf{C1}\cdot(\text{OTf})_2$ complexes at the 50% probability level. $\text{Cu}-\text{N}_{\text{naph}}$ and $\text{Cu}\cdots\text{Cu}$ distances (top), non-covalent interactions (middle) and naphthyridine bending angles (bottom). Solvent molecules, free anions and hydrogen atoms (except for the O-H bridges or when discussed) are omitted for clarity.

contrast, BF_4^- anions, lacking an oxygen-enriched structure, steer clear of the relatively acidic protons associated with both bis(μ -hydroxido) and pyrazolo bridges, as well as the naphthyridine moieties, primarily interacting with the methyl groups. It is noteworthy that, even though the distance differs only by a few Å, the electronic and steric hindrance for complex **C1**·(BF_4)₂ differs significantly from those of **C1**·(ClO_4)₂ and **C1**·(OTf)₂, allowing the coordination of solvent molecules to the copper(II) centers (Table S3, ESI[†]). Additionally, solvent molecules were found in the crystal structures of **C1**·(ClO_4)₂, **C1**·(BF_4)₂ and **C1**·(OTf)₂, showing the presence of acetone, water and tetrahydrofuran molecules, respectively. All these differences are reflected in the naphthyridine scaffold, which is shown to be bent out of the $\text{N}_{\text{naph}}\text{CuCuN}_{\text{naph}}$ plane by *ca.* 4.24°, 3.72° and 8.13° for **C1**·(ClO_4)₂, **C1**·(BF_4)₂ and **C1**·(OTf)₂, respectively. Within this context, it is noteworthy to mention that the nature of the anion plays a pivotal role not only with the **C1**²⁺ scaffold but also with these solvent molecules by allowing their proximity to the complex and trapping them into **C1**²⁺–anion pockets.

Interestingly, green crystals were also obtained by the slow evaporation of the acetonitrile solution recovered from the washings of **C1**·(OTf)₂. The single-crystal X-ray diffraction analysis revealed the unexpected formation of neutral mononuclear copper(II) complex **C2** as a side product (see Scheme S2 and proposed mechanism of formation for **C2** in the ESI[†]).

The previously reported naphthyridine-based dicopper(II,II) complex¹⁰ in CH_3CN solution with 100 mM [*n*-Bu₄N] ClO_4 shows an anion exchange of OTf^- by ClO_4^- . Then, in order to get further insights into these non-covalent interactions in solution, we analyzed the nature of the complex species under electrochemical conditions by determining their oxidative potentials, diffusion coefficients and hydrodynamic radii (Table S4, ESI[†]). One can expect an anion exchange process by perchlorates for both **C1**·(BF_4)₂ and **C1**·(OTf)₂ forming complex **C1**·(ClO_4)₂. Interestingly and contrary to our expectations, when analyzing the oxidation peak potentials for this

family of complexes (Fig. 2(a)), we observed that they appeared shifted to more anodic potentials following the trend $E_{\text{pa}}([\text{C1}\cdot(\text{ClO}_4)_2]) < E_{\text{pa}}([\text{C1}\cdot(\text{BF}_4)_2]) < E_{\text{pa}}([\text{C1}\cdot(\text{OTf})_2])$ and indicating that at least a few of these non-covalent interactions were maintained in solution, contrary to the reported behavior of the parent complex.^{9,11} From this, it can be inferred that (i) the inner **C1**²⁺ nature for each of these complexes is kept under electrochemical conditions and must be studied individually and (ii) higher oxidation potentials are observed for anions with higher hydrophobic character. Additionally, the significant differences in the current intensities exhibited by the different complexes show that they diffuse differently towards the working electrode (Table S4, ESI[†]). We hypothesize that this behavior could be attributed to the anions present in the complexes, whereby they could keep and/or establish ion-pair interactions affecting the 1st and 2nd coordination spheres of the complexes in solution. As already evidenced in the solid-state, the nature of the anion is responsible for bending the naphthyridine scaffold out of the $\text{N}_{\text{naph}}\text{CuCuN}_{\text{naph}}$ plane, diminishing both σ -donating and π -accepting electronic characters, which are translated towards higher oxidation potentials. More to this point, when such cyclic voltammetry was performed in CH_3CN solution with 100 mM [*n*-Bu₄N] BF_4 instead of [*n*-Bu₄N] ClO_4 , E_{pa} for both **C1**·(BF_4)₂ and **C1**·(OTf)₂ decreased *ca.* 140 mV and 190 mV, respectively, whereas that of **C1**·(ClO_4)₂ remained invariable (Fig. S20 and S21, ESI[†]). Under this scenario, $\text{Cu}^{\text{II}}\text{Cu}^{\text{III}}$ electro-generated species are favored and better stabilized by BF_4^- (electrolyte) anions for both **C1**·(BF_4)₂ and **C1**·(OTf)₂ complexes. These phenomena appear by the fact that changing a ClO_4^- environment by BF_4^- intrinsically shifts the nature of the non-covalent interactions from anion– π , $\text{O}-\text{H}\cdots\text{O}$ and $\text{C}-\text{H}\cdots\text{O}$ to mainly $\text{B}-\text{F}\cdots\text{H}-\text{C}$ interactions, which are more prompted to be established by **C1**·(BF_4)₂ and **C1**·(OTf)₂ rather than **C1**·(ClO_4)₂.

In addition to the electrochemical studies, the located spin density for the complexes prepared here was studied by electron paramagnetic resonance (EPR). Their spectra were recorded in anhydrous acetonitrile containing 0.1 M [*n*-Bu₄N] ClO_4 at 100 K (Table S4, ESI[†]). As shown in Fig. 2(b), all

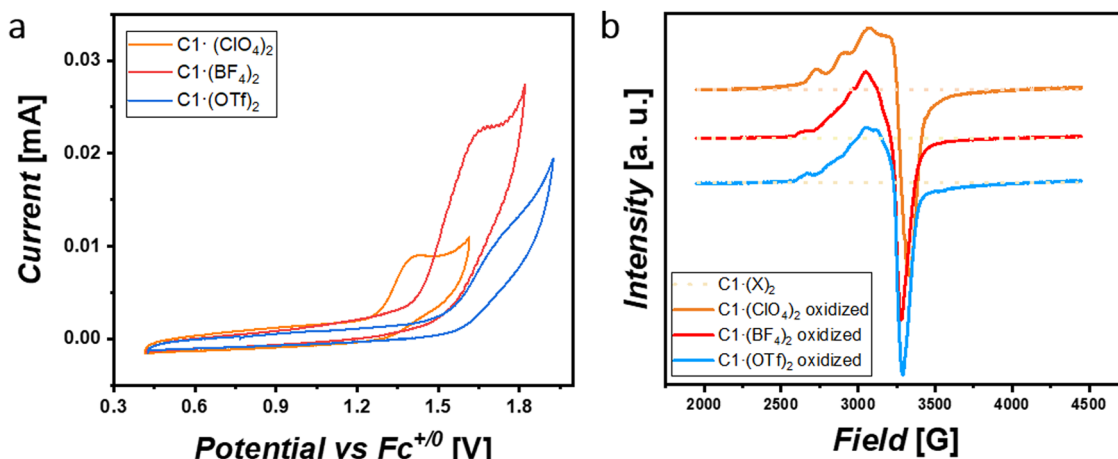


Fig. 2 (a) Cyclic voltammograms for 1 mM solutions of **C1**·(ClO_4)₂ (orange), **C1**·(BF_4)₂ (red) and **C1**·(OTf)₂ (blue) complexes in Ar-saturated anhydrous acetonitrile containing 0.1 M [*n*-Bu₄N] ClO_4 . Scan rate = 50 mV s⁻¹. (b) EPR spectra at 100 K for 1 mM solutions of **C1**·(ClO_4)₂ (orange), **C1**·(BF_4)₂ (red) and **C1**·(OTf)₂ (blue) before and after electrochemical mono-oxidation in Ar-saturated anhydrous acetonitrile containing 0.1 M [*n*-Bu₄N] ClO_4 .

complexes except **C2** (Fig. S23d, ESI[†]) exhibited a silent signal before oxidation pointing to the preservation of an antiferromagnetic behavior for the Cu^{II}Cu^{II} species. However, the **C1**-(X)₂ family showed X-band signals after electrochemically passing a charge of *ca.* 0.16 C (Fig. S22, ESI[†]) corresponding to mono-oxidation from Cu^{II}Cu^{II} to Cu^{II}Cu^{III} (Fig. 2(b)) for half of the complexes in solution. Interestingly, after simulating their monooxidized EPR spectra (Fig. S23, ESI[†]), we inferred that the three oxidized complexes exhibited a localized mixed-valent Cu^{II}Cu^{III} behaviour at 100 K. Furthermore, the small variations observed in such EPR spectra for the three monooxidized complexes suggest an influence related to the presence of solvent and anion molecules through non-covalent interactions (2nd sphere effects).

In summary, we have demonstrated that the anions present in dicopper(II,II) complexes bearing a naphthyridine scaffold are able to bend the latter decreasing both σ -donating and π -accepting electronic properties, while establishing non-covalent interactions (hydrogen bonding, anion- π , O \cdots C-H, C-H \cdots π , B-F \cdots H-C, S-O \cdots C-H and C-F \cdots H-C). Additionally, the presence of molecular pockets of dissimilar nature allows the accommodation of substrates like solvent molecules, a key step towards the development of a catalyst. Under this scenario, the anion nature dictates the availability of a pocket for a selected substrate. This was reflected in Cu^{III}/Cu^{II} oxidation potentials ranging from 1.36, 1.57 and 1.63 V *vs.* Fe^{+/-} and matched with the increasing hydrophobic characters for the ClO₄⁻, BF₄⁻ and OTf⁻ anions, respectively, in [nBu₄N]ClO₄/CH₃CN. Moreover, OTf⁻ led to the activation and promotion of C_{sp³}-N_{pyrazole} bond cleavage through non-covalent interactions (Scheme S2, ESI[†]).

To the best of our knowledge, this work represents a unique scenario where non-covalent interactions have been successfully unraveled. This evidence provides a fresh set of guidelines for the design and applicability of novel catalysts, showcasing the significance of these subtle forces, which should not be overlooked. These forces can persist and actively participate in solution reactions. Further investigations in the near future are

expected to delve into the role of the anion in C-H oxidation/oxygenation reactions.

This work was supported by the French Agence Nationale de la Recherche (ANR-22-CE07-0032). The authors are grateful to ICMG UAR 2607 for the analytical facilities (NMR, ESI-MS, EPR and X-Ray). This work has been partially supported by the CBH-EUR-GS (ANR-17-EURE-0003) and Labex ARCAINE (ANR-11-LABX-0003-01) programs, in the framework of which this work has been carried out. Dr Florian Molton and Rodolphe Gueret are acknowledged for EPR and HR-ESI-MS analyses, respectively. We kindly acknowledge Dr Nicolas Le Poul, Dr Marius Réglier and Dr Jalila Simaan for fruitful discussions.

Conflicts of interest

There are no conflicts to declare.

Notes and references

- 1 M. Y. Jin, Q. Zhen, D. Xiao, G. Tao, X. Xing, P. Yu and C. Xu, *Nat. Commun.*, 2022, **13**, 3276.
- 2 X. Lucas, A. Bauzá, A. Frontera and D. Quiñonero, *Chem. Sci.*, 2016, **7**, 1038.
- 3 A. Gehlhaar, C. Wölper, F. van der Vight, G. Jansen and S. Schultz, *Eur. J. Inorg. Chem.*, 2022, e202100883.
- 4 E. A. Meyer, R. K. Castellano and F. Diederich, *Angew. Chem., Int. Ed.*, 2003, **42**, 1210.
- 5 K. Müller-Dethlefs and P. Hobza, *Chem. Rev.*, 2000, **100**, 143.
- 6 E. H. Krenske and K. N. Houk, *Acc. Chem. Res.*, 2013, **46**, 979.
- 7 V. Mzozoyana, F. R. van Heerden and C. Grimmer, *Beilstein J. Org. Chem.*, 2020, **16**, 190.
- 8 M. Morisue, M. Kawanishi, I. Ueno, T. Nakamura, T. Nabeshima, K. Imamura and K. Nozaki, *J. Phys. Chem. B*, 2021, **125**, 9286.
- 9 R. A. Wong, Y. Yokota, M. Wakisaka, J. Inukai and Y. Kim, *Nat. Commun.*, 2020, **11**, 4194.
- 10 J. A. Isaac, F. Gennarini, I. López, A. Thibon-Pourret, R. David, G. Gellon, B. Gennaro, C. Philouze, F. Meyer, S. Demeshko, Y. Le Mest, M. Réglier, H. Jamet, N. Le Poul and C. Belle, *Inorg. Chem.*, 2016, **55**, 8263.
- 11 J. A. Isaac, A. Thibon-Pourret, A. Durand, C. Philouze, N. Le Poul and C. Belle, *Chem. Commun.*, 2019, **55**, 12711.
- 12 C. Vu, D. Walker, J. Wells and S. Fox, *J. Heterocycl. Chem.*, 2002, **39**, 829.
- 13 M. Tansky, Z. Gu and R. J. Comito, *J. Org. Chem.*, 2021, **86**, 1601.